

RESEARCH LETTER

10.1002/2016GL071205

Key Points:

- Underwater glider observes phytoplankton distribution in Antarctic coastal seas
- Glider data are used to determine ecologically relevant mixed-layer depth
- Maximum of buoyancy frequency is ecologically relevant mixed-layer depth

Supporting Information:

- Supporting Information S1
- Figure S1
- Figure S2

Correspondence to:

F. Carvalho,
filipa@marine.rutgers.edu

Citation:

Carvalho, F., J. Kohut, M. J. Oliver, and O. Schofield (2017), Defining the ecologically relevant mixed-layer depth for Antarctica's coastal seas, *Geophys. Res. Lett.*, *44*, doi:10.1002/2016GL071205.

Received 13 SEP 2016

Accepted 2 JAN 2017

Accepted article online 5 JAN 2017

©2017. The Authors.

This is an open access article under the terms of the Creative Commons Attribution-NonCommercial-NoDerivs License, which permits use and distribution in any medium, provided the original work is properly cited, the use is non-commercial and no modifications or adaptations are made.

Defining the ecologically relevant mixed-layer depth for Antarctica's coastal seas

Filipa Carvalho¹ , Josh Kohut¹ , Matthew J. Oliver² , and Oscar Schofield¹ 

¹Department of Marine and Coastal Sciences, Rutgers University, New Brunswick, New Jersey, USA, ²College of Earth, Ocean, and Environment, University of Delaware, Lewes, Delaware, USA

Abstract Mixed-layer depth (MLD) has been widely linked to phytoplankton dynamics in Antarctica's coastal regions; however, inconsistent definitions have made intercomparisons among region-specific studies difficult. Using a data set with over 20,000 water column profiles corresponding to 32 Slocum glider deployments in three coastal Antarctic regions (Ross Sea, Amundsen Sea, and West Antarctic Peninsula), we evaluated the relationship between MLD and phytoplankton vertical distribution. Comparisons of these MLD estimates to an applied definition of phytoplankton bloom depth, as defined by the deepest inflection point in the chlorophyll profile, show that the maximum of buoyancy frequency is a good proxy for an ecologically relevant MLD. A quality index is used to filter profiles where MLD is not determined. Despite the different regional physical settings, we found that the MLD definition based on the maximum of buoyancy frequency best describes the depth to which phytoplankton can be mixed in Antarctica's coastal seas.

1. Introduction

The surface mixed layer is a portion of the upper ocean where turbulent mixing processes form an upper density layer distinct from the layer below. The depth of these layers varies greatly across the world's ocean in time and space and plays an important role in interpreting the environmental factors driving phytoplankton blooms [Behrenfeld and Boss, 2014]. Mixed-layer depth (MLD) is therefore a central metric for understanding phytoplankton dynamics [Sverdrup, 1953] especially in Antarctica's coastal seas [Fragoso and Smith, 2012; Venables et al., 2013]. The depth of the surface mixed-layer can regulate the amount of solar radiation available to the phytoplankton community [Denman and Gargett, 1983; Mitchell et al., 1991]. From below, water column stability at the base of the ML has been linked to the flux of nutrients to the surface layer [Ducklow et al., 2007; Prézelin et al., 2000; Prézelin et al., 2004]. A recent study by Smith and Jones [2015] showed that vertical mixing and phytoplankton biomass in the Ross Sea are consistent with the critical depth concept formalized by Sverdrup [1953]. This critical depth is a function of incoming radiation, which in the poles shows a marked seasonality, and is an important factor controlling phytoplankton dynamics in polar seas [Smith and Sakshaug, 2013]. Similar conclusions relating the critical depth hypothesis with phytoplankton growth were found for the West Antarctic Peninsula [Carvalho et al., 2016; Cimino et al., 2016; Vernet et al., 2008].

While seasonal mixed-layers have been widely used to better understand the critical links between the physical structure of the water column and primary production, there are a wide range of methods and metrics used to estimate this important parameter. MLD calculations are based on temperature, salinity, or density. Common methods used in MLD calculations in Antarctic waters are based on either a difference or gradient in the target variable, and every study justifies their specific method. Estimates of MLD from a difference measured at two depths use a range of values. Temperature thresholds vary from 0.8°C [Kara et al., 2000] to 0.2°C [de Boyer Montégut et al., 2004; Dong et al., 2008], while potential density thresholds vary from 0.01 kg m⁻³ [Smith and Jones, 2015], 0.03 kg m⁻³ [Sallée et al., 2010], and 0.05 kg m⁻³ [Venables et al., 2013]. The reference depths over which these differences are estimated can vary from the near surface [Venables et al., 2013] to as deep as 10 m [Smith and Jones, 2015]. All these differences in criteria and method can potentially yield different estimates of MLD. This is especially troublesome when trying to compare results between studies and distributed seas within which local physical conditions lead to different optimal methods to estimate local MLD. In this study, we use concurrent profiles of hydrography and chlorophyll *a* (chl *a*) fluorescence during the austral spring/summer season in three coastal regions around Antarctica and propose a standard and ecologically relevant metric of

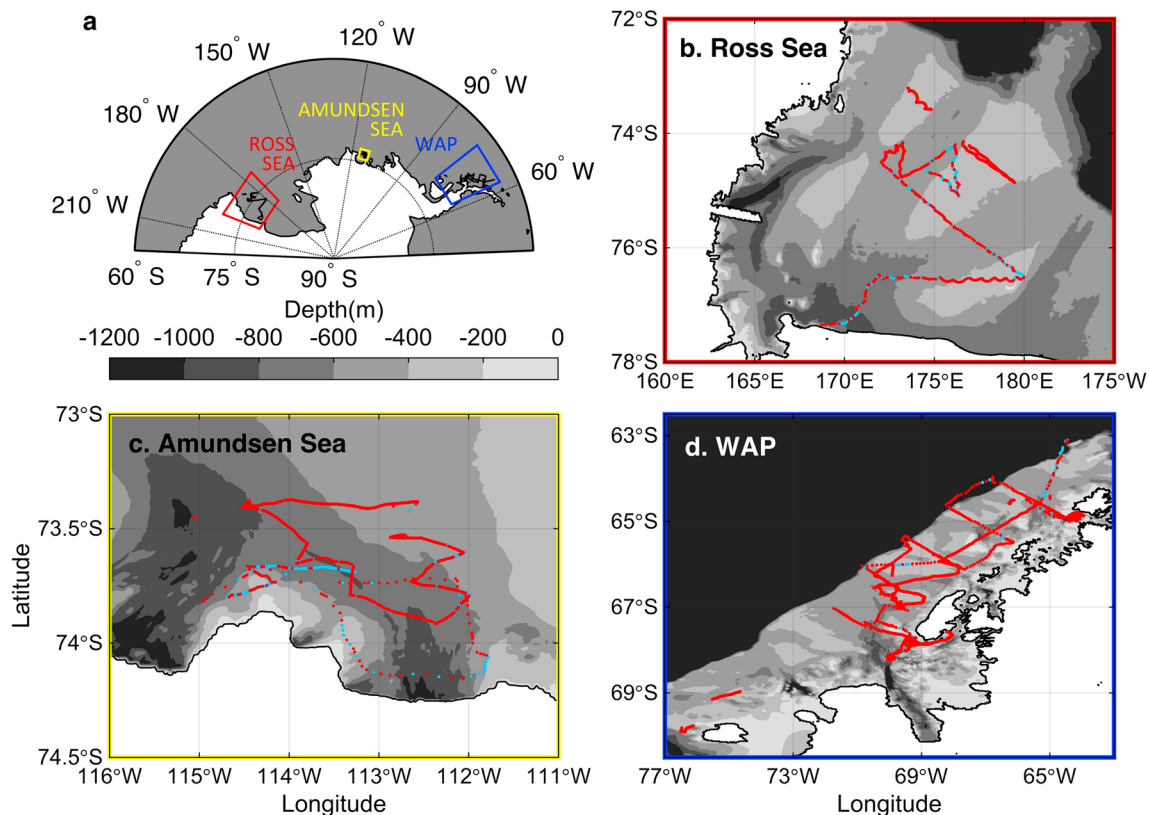


Figure 1. Location of glider data used in the analysis: (a) glider tracks in the three main regions. (b–d) Bathymetry maps overlaid with the detailed location of each individual glider profile (dots) for the regions shown in Figure 1a: (b) Ross Sea, (c) Amundsen Sea, and (d) WAP. Red dots: MLD quality index (QI) > 0.5 (see section 2.2 for details); blue dots: remaining profiles not considered for the MLD analysis (QI < 0.5).

MLD as it consistently captures the lower vertical limit of phytoplankton distribution across the Amundsen Sea (AS), the Ross Sea (RS), and the shelf along the Western Antarctic Peninsula (WAP) that facilitate comparisons between studies.

2. Data and Methods

2.1. Slocum Gliders

Slocum electric gliders are 1.5 m torpedo-shaped buoyancy-driven autonomous underwater vehicles that provide high-resolution surveys of the physical and bio-optical properties of the upper water column [Schofield *et al.*, 2007]. All gliders used in this analysis were equipped with a Seabird conductivity-temperature-depth (CTD) sensor and carried WET Labs Inc. Environmental Characterization Optics (ECO) pucks, which measured chl *a* fluorescence. Glider-based conductivity, temperature, and depth measurements were compared with a calibrated ship CTD sensor on deployment and recovery to ensure data quality, as well as with a calibrated laboratory CTD prior to deployment (as described in Kohut *et al.* [2014]). Each glider profile was averaged into 1 m bins and assigned a midpoint latitude and longitude. Only profiles with 50 bins or more were considered for the analysis. Glider profiles start at 2–4 m depth. In the AS, three missions collected 2247 profiles (December 2010 to February 2011 and January 2015). In the RS, three missions collected 2212 profiles (December 2010 to January 2011). Along the WAP, 26 missions collected 16,673 profiles (December–March, 2009 through 2015). Overall, these data include 21,132 profiles, 465 days at sea and 9836 km flown during the austral spring/summer (Figure 1).

2.2. Mixed-Layer Depth

We evaluated an ecologically relevant MLD definition based on comparisons with concurrent chl *a* fluorescence profiles (described below). We show a detailed analysis on the MLD estimated based

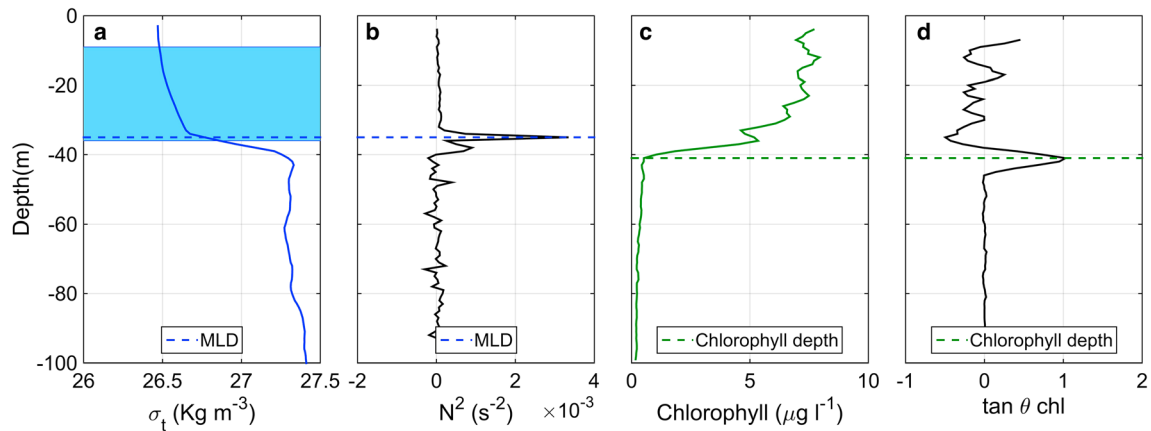


Figure 2. Determination of mixed-layer depth (MLD) and chl *a* depth (Z_{chl}) from a glider profile (located at 64.827°S, 64.286°W at GMT 4:29 on 6 January 2014). (a) Density profile (solid blue line) with MLD (blue dashed line) calculated by max (N^2) and range of MLD (shaded blue) calculated using methods described in Table 1; (b) calculated buoyancy frequency (N^2) profile and MLD; (c) chl *a* profile (solid green line) with Z_{chl} (green dashed line) defined by the maximum angle method [Chu and Fan, 2011], or the max ($\tan\theta_{(chl)}$), and (d) calculated $\tan\theta_{(chl)}$ and Z_{chl} .

on the maximum of buoyancy frequency ($\max(N^2)$ or stability frequency). For each profile (Figures 2a and 2b), MLD was determined by finding the depth of the maximum water column buoyancy frequency. The same analysis was conducted for the most commonly used estimates of MLD in Antarctica’s coastal seas and presented in the supporting information as a comparison against our proposed MLD definition.

The determination of MLD is based on the principle that there is a near-surface layer characterized by quasi-homogeneous properties with a standard deviation of the property within this layer close to zero. Below the MLD, the variance of the property should increase rapidly. To clarify the relationship between MLD and chl *a* in such a high-resolution data set, a quality index (QI) (equation (1)) by Lorbacher *et al.* [2006] was used to evaluate our MLD calculations and filter out profiles where MLD could not be resolved:

$$QI = 1 - \frac{\text{rmsd}(\rho_k - \bar{\rho})|_{(Z_1, Z_{MLD})}}{\text{rmsd}(\rho_k - \bar{\rho})|_{(Z_1, 1.5 \times Z_{MLD})}} \quad (1)$$

where ρ_k is the density at a given depth (k), Z_1 is the first layer near the surface, and $\text{rmsd}()$ denotes the standard deviation from the vertical mean $\bar{\rho}$ from Z_1 either to the MLD or $1.5 \times \text{MLD}$. This index evaluates the quality of the MLD computation. Using this, MLDs can be characterized into estimates determined with certainty ($QI > 0.8$), determined but with some uncertainty ($0.5 < QI < 0.8$) or not determined ($QI < 0.5$). Example of profiles for data removed from the analysis ($QI < 0.5$) can be found in the supporting information (Figure S2). This QI metric does not consider the strength of stratification, just homogeneity of the surface layer above the defined MLD. Therefore, by definition, the MLD estimate is close to the lower boundary of that vertically uniform layer. Following the thresholds set by Lorbacher *et al.* [2006], for the analyses presented in this study, a quality index of 0.5 was used to reasonably warrant a calculation of MLD. The quality index threshold of 0.5 was determined based on the insensitivity of the slope of the trend lines using higher QI values (0.8).

Apart from the depth of the ML, stratification also plays an important role in phytoplankton dynamics [Holm-Hansen and Mitchell, 1991; Mitchell *et al.*, 1991]. The differences in the vertical physical structure setting seen in the temperature (T) and salinity (S) plots (Figure 3) result in differences in stratification. To identify the profiles with the highest stability at the base of the MLD in each region, stability was normalized independently for each region by dividing the buoyancy frequency at the base of MLD of that profile by the regional average of buoyancy frequency at the base of the MLD. The normalized stability was calculated to find the magnitude of each point as it relates to the overall stability in each region. This allows the regional differences due to the vertical structure of the water column to be removed.

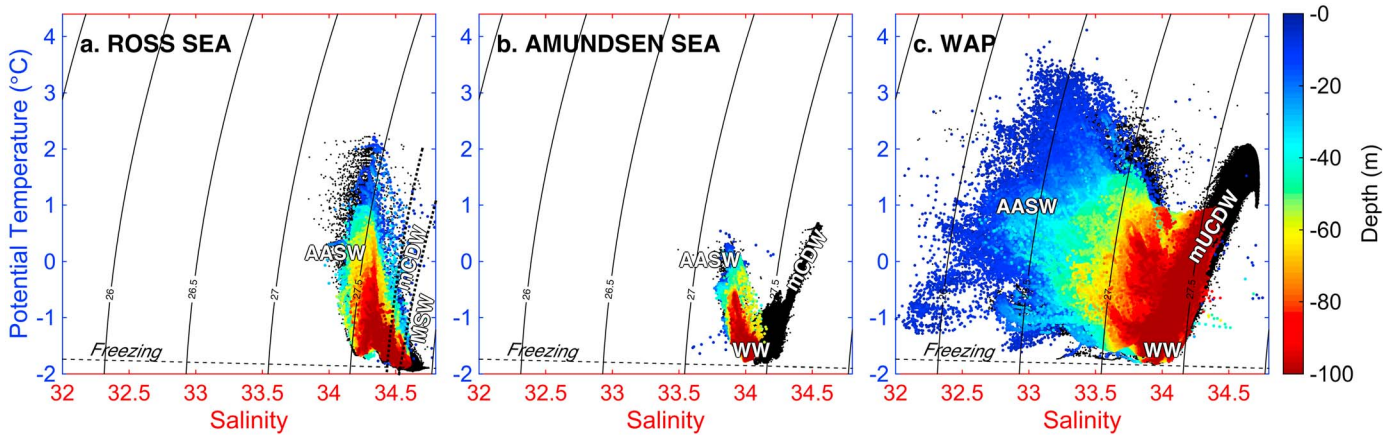


Figure 3. The θ - S scatter plots for all three areas shown in Figure 1: (a) Ross Sea, (b) Amundsen Sea, and (c) WAP. Color indicates depth of the water column measurement in the upper 100 m of the water column. All data between 100 and 1000 m are plotted in black. Primary water masses sampled are indicated and labeled (WW = Winter Water; MSW = Modified Shelf Water; AASW = Antarctic (summer) Surface Water; mUCDW = modified Upper Circumpolar Deep Water).

2.3. Chlorophyll *a* Fluorescence

Chl *a* fluorescence, as measured by the glider ECO pucks, is our indicator of phytoplankton biomass. Discrete in situ water samples were collected from several depths from casts during each glider deployment and recovery. Water samples were filtered onto 25 mm Whatman GF/F filters and extracted using 90% acetone, and chl *a* concentration was then measured using a fluorometer. For each deployment, the structure and magnitude of chl *a* measured by the glider puck was verified against both the independent discrete measurements and an independent calibrated fluorometer deployed from a collocated ship station. While the complex relation between fluorescence versus biomass was not fully evaluated, we provide an accurate characterization of the observed fluorescence, fully realizing that our measurements may not accurately represent phytoplankton biomass. Also, since our analysis focuses on the bottom of the phytoplankton biomass layer, daily nonphotochemical quenching of chl *a* fluorescence is not a factor in our analysis.

Following a method adapted from the maximum angle principle used to calculate MLD [Chu and Fan, 2011], the depth of lower boundary of chl *a* was estimated, referred to as chlorophyll depth (Z_{chl}) in the analysis. This method is based on three main steps: (1) fitting the profile data with a vector (pointing downward and with n points) from shallower depths to a certain depth k and a second vector from that depth to deeper depth ($k + 1 + n$); (2) identifying the tangent angle ($\tan\theta$) between the two vectors for each depth k ; and (3) defining the MLD by determining the maximum angle in each profile. Here we apply the same principle using the maximum angle, as we are interested in calculating the depth of the deepest inflection point in the chl *a* profile. Using a vector of $n = 7$ data points, the depth of the $\max(\tan\theta)$ of the chl *a* profile was determined and used as the Z_{chl} (Figures 2c and 2d). A quality index (QC) (equation (2)) was also applied to the chlorophyll data to evaluate the Z_{chl} computation. A modification to equation (1) was made to account for the homogeneity occurring below the Z_{chl} and not above:

$$QC = 1 - \frac{\text{rmsd}(\text{CHL}_k - \overline{\text{CHL}})|_{(Z_{chl}, Z_D)}}{\text{rmsd}(\text{CHL}_k - \overline{\text{CHL}})|_{(Z_D - 1.5(Z_D - Z_{chl}), Z_D)}} \quad (2)$$

As both variables have errors in them and linear relationships are expected between both variables [Holm-Hansen and Mitchell, 1991; Mitchell et al., 1991], model 2 regressions were applied to concurrent MLD and Z_{chl} calculations to evaluate the MLD determination of the definitions chosen by comparing it to a 1:1 line.

3. Results and Discussion

Each region had a different distribution of water masses as indicated in temperature (T) and salinity (S) space (Figure 3). Surface water in the RS and AS were similar, but quite different from the WAP while at depth, AS and WAP showed similarities. Compared to the WAP, both Ross and Amundsen Seas showed overall colder and saltier waters with the latter being on average saltier. The warmer, saltier and deep modified Upper

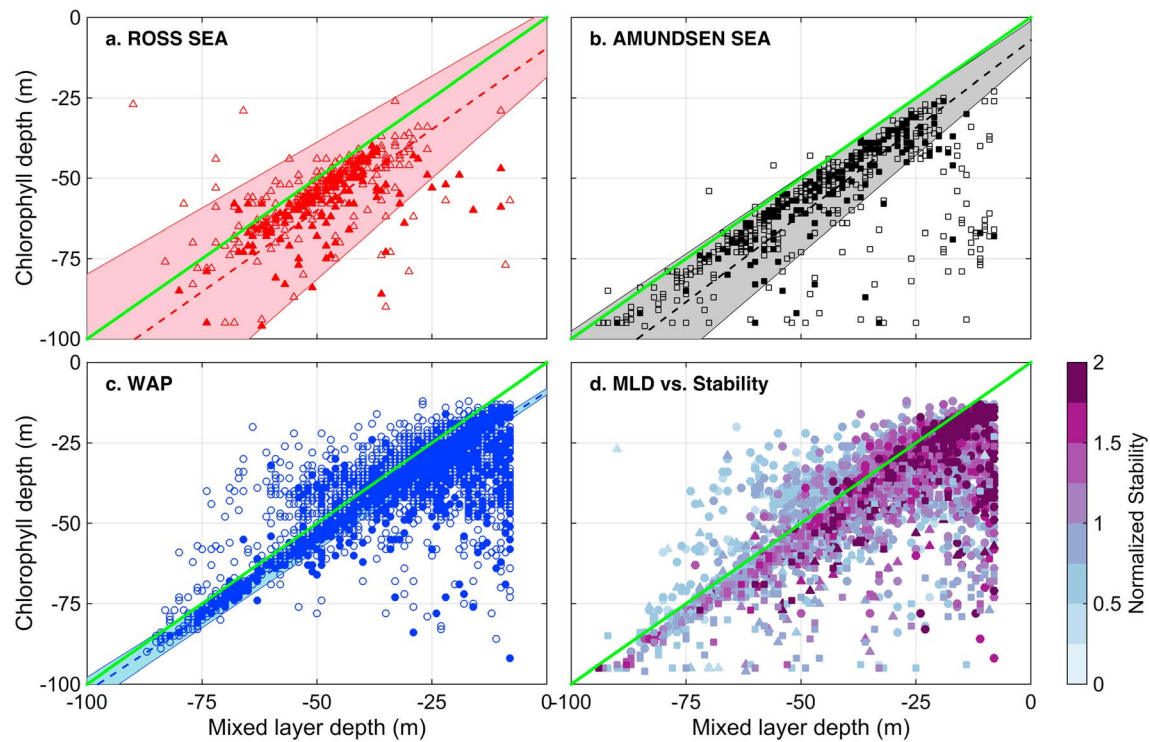


Figure 4. Correlation between MLD and Z_{chl} for all glider profiles with quality index (QI) over 0.5 (open marker) and over 0.8 (filled marker) for all three regions: (a) Ross Sea (triangle); (b) Amundsen Sea (square); (c) WAP (circle); (d) comparison between all three Antarctic regions (QI > 0.5) with normalized stability frequency colored. Ninety-five percent confidence intervals (shaded area) and model 2 regression line are shown for QI > 0.8 (dashed line). A quality index of 0.5 was also applied to chl a (QI_{chl}) profiles, and only profiles with $QI_{chl} > 0.5$ are shown above. Line 1:1 is shown in green.

Circumpolar Deep Water (mUCDW) found at shallower depths in the WAP was not seen in the upper 100 m (colored dots in Figure 3) in RS and AS. In both the latter regions, T_{min} was found generally in the deepest sampled waters (red). The WAP (Figure 3c), with the widest range of T-S properties as it is located at lower latitudes, spans entire seasonal cycles due to more sustained sampling and is more influenced by coastal inputs.

We compared our MLD estimation based on N^2 and chlorophyll depth, described in section 2.3, across each of the coastal regions. Profiles with QI and QC values less than 0.5 [Lorbacher *et al.*, 2006] were removed as MLD and Z_{chl} were not clearly defined. The remaining profiles were characterized as “estimated with uncertainty” ($0.5 < QI < 0.8$; Figure 4, open markers) and “estimated with certainty” ($QI > 0.8$; Figure 4, filled markers). A linear, model 2 regression was applied to each regional data set, and the line and corresponding R^2 are reported in the supporting information (Table S2). Although some regional differences were found in the MLD ranges, all three regions showed an MLD-chl a relationship close to 1:1 with 95% confidence (compare dashed trend lines with green), i.e., the deeper the MLD, the deeper the lower boundary of the chl a profile. The observed differences in the depth of the ML across regions (Figure 4) were mostly influenced by the timing of the measurements, i.e., uneven sampling in time in different regions. Nevertheless, the MLD calculations are within range of those reported for each region [Schofield *et al.*, 2015; Smith *et al.*, 2014; Vernet *et al.*, 2008].

Given the disproportionately greater number of profiles collected in the WAP (Figure 4c), this region showed the widest range of MLDs estimated with certainty ($QI > 0.8$) of all three regions, ranging from 8 to 65 m of depth. It showed, on average, the shallowest MLD ($\overline{MLD} = -33\text{ m} \pm 13$) and a trend line ($y = 0.93175x - 9.0415$; $R^2 = 0.82$; $p < 0.0001$) close to the 1:1 line (green line). The RS (Figure 4a) showed the deepest MLD ($\overline{MLD} = -49\text{ m} \pm 9$), but regardless, the relationship between MLD and chl a ($y = 1.0098x - 9.5745$; $R^2 = 0.60$; $p < 0.0001$) was similar to those seen in the other two regions. The AS that exhibited the smallest number of data points, however, showed a high R^2 ($y = 1.0849x - 7.125$; $R^2 = 0.78$;

Table 1. Examples of Criteria Used to Define MLD in Waters Around Antarctica

Author	Area studied	MLD Threshold Criterion
<i>Kara et al.</i> [2000]	Global ocean	$\Delta T = 0.8^\circ\text{C}\Delta\sigma_\theta = \sigma_\theta(T + \Delta T, S) - \sigma_\theta(T, S)$ with $\Delta T = 0.8^\circ\text{C}$
<i>de Boyer Montégut et al.</i> [2004]	Global ocean	$\Delta T = 0.2^\circ\text{C}\Delta\sigma_\theta = 0.03 \text{ kg m}^{-3}$
<i>Dong et al.</i> [2008]	Southern Ocean (open ocean)	$\Delta\rho = 0.03 \text{ kg m}^{-3} \Delta T = 0.2^\circ\text{C}$
<i>Sallée et al.</i> [2010]	Southern Ocean (open ocean)	$\Delta\sigma_\theta = 0.03 \text{ kg m}^{-3}$
<i>Long et al.</i> [2012]	Ross Sea	$\Delta\sigma_\theta = 0.05 \text{ kg m}^{-3}$
<i>Smith and Jones</i> [2015]	Ross Sea	$\Delta\sigma_\theta = 0.01 \text{ kg m}^{-3}$
<i>Fragoso and Smith</i> [2012]	Ross and Amundsen Seas	$\Delta\sigma_\theta = 0.01 \text{ kg m}^{-3}$
<i>Schofield et al.</i> [2015]	Amundsen Sea	$\max(N^2)$
<i>Vernet et al.</i> [2008]; <i>Prézelin et al.</i> [2004]	WAP	Not specified
<i>Venables et al.</i> [2013]	Margarite Trough (WAP)	$\Delta\sigma_\theta = 0.05 \text{ kg m}^{-3}$
<i>Moline et al.</i> [1997]; <i>Cimino et al.</i> [2016]	Anvers Island (WAP)	$\max(\partial\rho/\partial z)$
<i>Walsh et al.</i> [2001]	Northern WAP	Not specified
<i>Mitchell and Holm-Hansen</i> [1991]	SW Bransfield Strait (WAP) and Drake Passage	$\Delta\sigma_\theta = 0.05 \text{ kg m}^{-3}$ (in 5 m window)

$p < 0.0001$) for both quality indices used. This region shows again a wider range of MLD comparatively to the Ross Sea, but has also, on average, deeper MLDs ($\overline{MLD} = -41 \text{ m} \pm 13$) than the WAP. All three regions showed slopes not significantly different than the 1:1 line (Table S2).

Comparing the trends obtained using both indices (QI > 0.8 compared to QI > 0.5, corresponding to 26–31% and 80–87% of the profiles, respectively) showed little differences (Table S2). Higher QIs are observed during summer and fall, where sharp gradients at the base of the seasonal mixed layer are present [*Lorbacher et al.*, 2006]. A maximum MLD difference of 3 m for the AS was observed when using QI > 0.5 compared to a higher MLD quality index, QI > 0.8; and overall, this difference was much smaller for the remaining two regions. This ensures that even though we are using a lower quality index to include more data in the analysis (QI > 0.5, the minimum threshold set by *Lorbacher et al.* [2006] for determining MLD), we are capturing the same patterns. Points that are closer to the trend line show, on average, much higher water stability (Figure 4d), with the shallowest MLD showing the highest water stability due to freshwater input from meltwater [*Martinson and Iannuzzi*, 1998]. Since our gliders measurements start at a minimum of 2 m depth and our Z_{chl} computation relies on a 7-point vector, it was not possible to evaluate the biophysical relationship in this study within the upper 7 m. This is a constraint on our method of evaluating the correlation between MLD and chlorophyll depth and not on the actual MLD determination. Studies in the region have also shown that most Z_{chl} occur deeper than 7 m [*Moline et al.*, 1997; *Smith et al.*, 2013]. Note that, as this method captures the maximum stability frequency of the water column profile, its accuracy depends both on the vertical resolution and the vertical extent of the measurements. This is especially important in the presence of meltwater lenses in the surface layer, which our gliders were not able to capture. This method relies on the implicit assumption of a two-layer ocean. Cases where the surface ocean has a well-defined (and deeper) ML and a surface active mixing layer [*Brainerd and Gregg*, 1995], this method will capture the depth of the strongest water column stability and therefore a lower QI may be determined based on this two-step surface ML if the base of the ML has a stronger N^2 value.

To determine the value of our combined method linking physical MLD with chl a depth, we evaluated several MLD methodologies. The most commonly used MLD criteria in polar waters (Table 1) were tested for each individual profile and matched against the Z_{chl} . The range of MLD calculated using the different criteria are presented for a representative profile as the shaded area in Figure 2a.

Using a model 2 linear regression, we were able to evaluate the various MLD definitions (Table S1 and Figure S1 in the supporting information) and concluded that the most ecologically relevant MLD determination method across all regions based on the strength of the correlation with the lower boundary of the chl a profile was the maximum of buoyancy frequency (section 2).

Independent of the different water mass compositions and dynamics present in each region, the biophysical relationship between MLD and chl a remains the same in all three regions. With slopes not significantly

different from the 1:1 line (within the 95% confidence intervals of the model 2 regression fit) in all three regions suggests that the MLD definition we are using is a good predictor of the depth of the inflection point in the chl *a* profile (lower boundary of the chl *a* patch in the water column) and is therefore an important parameter in phytoplankton dynamics studies.

4. Conclusions

Understanding the spatial and temporal variability of phytoplankton is important, especially to assess ecological dynamics of marine food webs. Historically different MLD calculations have been applied in Antarctic continental shelves and linked to phytoplankton dynamics [Mitchell and Holm-Hansen, 1991; Smith and Jones, 2015; Vernet *et al.*, 2008]. These calculations were based on different subjective thresholds (sometimes linked to local hydrography) for the same regions. This leads to significant variability in MLD estimations, making comparisons between studies and regions problematic. MLDs calculated from buoyancy frequency were similarly correlated with our adapted estimate of Z_{chl} across all three coastal regions. Given the variability in water mass distribution and volume between the RS, AS, and along the WAP, this biophysical relationship was similar in all regions, which suggests that the maximum of stability frequency (or $\max(N^2)$) is an appropriate and robust metric to compare and contrast biophysical processes across all three Antarctic regions.

Acknowledgments

We thank the crews of R/V Nathaniel B. Palmer, ARSV Laurence M. Gould, R/V Araon, Palmer Station support staff, and the Rutgers glider team for facilitating our long-term data collection efforts. We also wish to thank five anonymous reviewers for their suggestions regarding the analysis in this paper. The research was supported by the National Science Foundation grants ANT-0823101 (Palmer-LTER), ANT-1327248, and ANT-1326541 (CONVERGE), ANT-0839039 (SEAFARERS), ANT-0838995 (ASPIRE), and the Korean Polar Research Institute grant PP1502 (KOPRI). Filipa Carvalho was funded by a Portuguese doctoral fellowship from Fundação para a Ciência e Tecnologia (DFRH - SFRH/BD/72705/2010). Glider data can be accessed at ERDDAP server at <http://erddap.marine.rutgers.edu/erddap/info/>.

References

- Behrenfeld, M. J., and E. S. Boss (2014), Resurrecting the ecological underpinnings of ocean plankton blooms, *Annu. Rev. Mar. Sci.*, *6*, 167–194.
- Brainerd, K. E., and M. C. Gregg (1995), Surface mixed and mixing layer depths, *Deep Sea Res., Part I*, *42*(9), 1521–1543.
- Carvalho, F., J. Kohut, M. J. Oliver, R. M. Sherrell, and O. Schofield (2016), Mixing and phytoplankton dynamics in a submarine canyon in the West Antarctic Peninsula, *J. Geophys. Res. Oceans*, *121*, 5069–5083, doi:10.1002/2016jc011650.
- Chu, P. C., and C. W. Fan (2011), Maximum angle method for determining mixed layer depth from seaglider data, *J. Oceanogr.*, *67*(2), 219–230, doi:10.1007/s10872-011-0019-2.
- Cimino, M. A., M. A. Moline, W. R. Fraser, D. L. Patterson-Fraser, and M. J. Oliver (2016), Climate-driven sympatry may not lead to foraging competition between congeneric top-predators, *Sci. Rep.*, *6*, doi:10.1038/srep18820.
- de Boyer Montégut, C., G. Madec, A. S. Fischer, A. Lazar, and D. Iudicone (2004), Mixed layer depth over the global ocean: An examination of profile data and a profile-based climatology, *J. Geophys. Res.*, *109*, C12003, doi:10.1029/2004JC002378.
- Denman, K., and A. Gargett (1983), Time and space scales of vertical mixing and advection of phytoplankton in the upper ocean, *Oceanography*, *28*(5), 801–815.
- Dong, S., J. Sprintall, S. T. Gille, and L. Talley (2008), Southern Ocean mixed-layer depth from Argo float profiles, *J. Geophys. Res.*, *113*, C06013, doi:10.1029/2006JC004051.
- Ducklow, H. W., K. Baker, D. G. Martinson, L. B. Quetin, R. M. Ross, R. C. Smith, S. E. Stammerjohn, M. Vernet, and W. Fraser (2007), Marine pelagic ecosystems: The west antarctic peninsula, *Philos. Trans. R. Soc. Lond. B Biol. Sci.*, *362*(1477), 67–94.
- Fragoso, G. M., and W. O. Smith (2012), Influence of hydrography on phytoplankton distribution in the Amundsen and Ross Seas, Antarctica, *J. Mar. Syst.*, *89*(1), 19–29, doi:10.1016/j.jmarsys.2011.07.008.
- Holm-Hansen, O., and B. Mitchell (1991), Spatial and temporal distribution of phytoplankton and primary production in the western Bransfield Strait region, *Deep Sea Res. Part A. Oceanogr. Res. Pap.*, *38*(8), 961–980.
- Kara, A. B., P. A. Rochford, and H. E. Hurlburt (2000), An optimal definition for ocean mixed layer depth, *J. Geophys. Res.*, *105*, 16,803–16,821, doi:10.1029/2000JC900072.
- Kohut, J., C. Haldeman, and J. Kerfoot (2014), Monitoring dissolved oxygen in New Jersey Coastal waters using autonomous gliders, *Tect. EPA/600/R-13/180*, U.S. Environmental Protection Agency, Washington, D. C.
- Long, M. C., L. N. Thomas, and R. B. Dunbar (2012), Control of phytoplankton bloom inception in the Ross Sea, Antarctica, by Ekman restratification, *Global Biogeochem. Cycles*, *26*, GB1006, doi:10.1029/2010GB003982.
- Lorbacher, K., D. Dommengot, P. P. Niiler, and A. Köhl (2006), Ocean mixed layer depth: A subsurface proxy of ocean-atmosphere variability, *J. Geophys. Res.*, *111*, C07010, doi:10.1029/2003JC002157.
- Martinson, D. G., and R. A. Iannuzzi (1998), Antarctic Ocean-Ice Interaction: Implications from Ocean Bulk Property Distributions in the Weddell Gyre, in *Antarctic Research Series, Antarctic Sea Ice: Physical Processes, Interactions and Variability*, edited by M. Jeffries, pp. 243–271, AGU, Boston, Mass.
- Mitchell, B. G., and O. Holm-Hansen (1991), Observations of modeling of the Antarctic phytoplankton crop in relation to mixing depth, *Deep Sea Res. Part A. Oceanogr. Res. Pap.*, *38*(8), 981–1007.
- Mitchell, B. G., E. A. Brody, O. Holm-Hansen, C. McClain, and J. Bishop (1991), Light limitation of phytoplankton biomass and macronutrient utilization in the Southern Ocean, *Limnol. Oceanogr.*, *36*(8), 1662–1677.
- Moline, M. A., B. B. Prezelin, O. Schofield, and R. C. Smith (1997), Temporal dynamics of coastal Antarctic phytoplankton: Environmental driving forces and impact of 1991/92 summer diatom bloom on the nutrient regimes, in *Antarctic Communities: Species, Structure and Survival*, edited by B. Battaglia, J. Valencia, and D. W. H. Walton, pp. 67–72, Cambridge Univ. Press, Cambridge.
- Prézelin, B. B., E. E. Hofmann, C. Mengelt, and J. M. Klinck (2000), The linkage between Upper Circumpolar Deep Water (UCDW) and phytoplankton assemblages on the west Antarctic Peninsula continental shelf, *J. Mar. Res.*, *58*(2), 165–202.
- Prézelin, B. B., E. E. Hofmann, M. Moline, and J. M. Klinck (2004), Physical forcing of phytoplankton community structure and primary production in continental shelf waters of the Western Antarctic Peninsula, *J. Mar. Res.*, *62*(3), 419–460.
- Sallée, J. B., K. G. Speer, and S. R. Rintoul (2010), Zonally asymmetric response of the Southern Ocean mixed-layer depth to the Southern Annular Mode, *Nat. Geosci.*, *3*(4), 273–279, doi:10.1038/ngeo812.

- Schofield, O., et al. (2007), Slocum gliders: Robust and ready, *J. Field Robot.*, 24(6), 473–485, doi:10.1002/rob.20200.
- Schofield, O., T. Miles, A.-C. Alderkamp, S. Lee, C. Haskins, E. Rogalsky, R. Sipler, R. M. Sherrell, and P. L. Yager (2015), In situ phytoplankton distributions in the Amundsen Sea Polynya measured by autonomous gliders, *Elementa: Sci. Anthropocene*, 3(1), 000,073.
- Smith, W., and R. M. Jones (2015), Vertical mixing, critical depths, and phytoplankton growth in the Ross Sea, *ICES J. Mar. Sci.: J. du Conseil*, 72(6), 1952–1960, doi:10.1093/icesjms/fsu234.
- Smith, W., and E. Sakshaug (2013), 9. Polar phytoplankton, in *Polar Oceanography: Chemistry, Biology, and Geology*, edited by W. Smith, pp. 477–526, Acad. Press, San Diego, Calif.
- Smith, W., S. Tozzi, M. C. Long, P. N. Sedwick, J. A. Peloquin, R. B. Dunbar, D. A. Hutchins, Z. Kolber, and G. R. DiTullio (2013), Spatial and temporal variations in variable fluorescence in the Ross Sea (Antarctica): Oceanographic correlates and bloom dynamics, *Deep Sea Res., Part I*, 79, 141–155.
- Smith, W., D. G. Ainley, K. R. Arrigo, and M. S. Dinniman (2014), The oceanography and ecology of the Ross Sea, *Annu. Rev. Mar. Sci.*, 6, 469–487.
- Sverdrup, H. (1953), On conditions for the vernal blooming of phytoplankton, *J. Conseil*, 18(3), 287–295.
- Venables, H. J., A. Clarke, and M. P. Meredith (2013), Wintertime controls on summer stratification and productivity at the western Antarctic Peninsula, *Limnol. Oceanogr.*, 58(3), 1035–1047.
- Vernet, M., D. Martinson, R. Iannuzzi, S. Stammerjohn, W. Kozlowski, K. Sines, R. Smith, and I. Garibotti (2008), Primary production within the sea-ice zone west of the Antarctic Peninsula: I—Sea ice, summer mixed layer, and irradiance, *Deep Sea Res., Part II*, 55(18-19), 2068–2085, doi:10.1016/j.dsr2.2008.05.021.
- Walsh, J. J., D. A. Dieterle, and J. Lenos (2001), A numerical analysis of carbon dynamics of the Southern Ocean phytoplankton community: The roles of light and grazing in effecting both sequestration of atmospheric CO₂ and food availability to larval krill, *Deep Sea Res., Part I*, 48(1), 1–48.